

1 **Title:** Interferons drive development of novel interleukin-15-responsive macrophages

2 **Running Title:** Novel macrophages respond to IL-15

3

4 **Authors and Affiliations:**

5 Scott M. Gordon^{*,§}, Mailyn A. Nishiguchi[§], Julie M. Chase[¶], Sneha Mani[#], Monica A. Mainigi[#],
6 and Edward M. Behrens^{§,¶}

7 ^{*}Division of Neonatology, Children's Hospital of Philadelphia, Philadelphia, PA 19104, USA,

8 [§]Perelman School of Medicine, University of Pennsylvania, Philadelphia, PA 19104, USA,

9 [¶]Division of Rheumatology, Children's Hospital of Philadelphia, Philadelphia, PA 19104, USA,

10 [#]Center for Research on Reproduction and Women's Health, University of Pennsylvania,
11 Philadelphia, PA 19104, USA

12

13 Address correspondence and reprint requests to Dr. Edward M. Behrens, Children's Hospital of
14 Philadelphia, 3615 Civic Center Blvd, Room 1107A ARC, Philadelphia, PA 19107. Office Phone:
15 215-590-7180, Office Fax: Fax: 215-590-1258, Email: behrens@email.chop.edu.

16

17 This work was supported by NIH grant R01 AI121250-A1 (E.M.B.), NIH grant T32 AI 118684
18 (S.M.G.), NIH grant T32 GM 008216 (M.A.N.), the Section on Neonatal-Perinatal Medicine of
19 the American Academy of Pediatrics, the Children's Hospital of Philadelphia Research Institute,
20 and the Division of Neonatology of Children's Hospital of Philadelphia (S.M.G.); Penn University
21 Research Foundation and March of Dimes Prematurity Research Center at the University of
22 Pennsylvania (M.A.M.).

23

24 S.M.G., M.A.N., J.M.C., and S.M. performed experiments. S.M.G. and E.M.B. wrote the
25 manuscript. M.A.N., J.M.C., S.M., and M.A.M. critically reviewed the manuscript.

26

27 The authors have declared that no conflict of interest exists.

28

29 The microarray data presented in this article have been submitted to the Gene Expression

30 Omnibus (<http://www.ncbi.nlm.nih.gov/geo/>) under accession number GSE132353.

31 **ABSTRACT**

32 Disruption in homeostasis of interleukin-15 (IL-15) is linked to poor maternal and fetal outcomes
33 during pregnancy. The only cells described to respond to IL-15 at the early maternal-fetal interface
34 have been natural killer (NK) cells. We now show a novel population of macrophages, evident in
35 several organs but enriched in the uterus of mice and humans, expressing the β chain of the IL-15
36 receptor complex (CD122) and responding to IL-15. CD122+ macrophages (CD122+Macs) are
37 morphologic, phenotypic, and transcriptomic macrophages that can derive from bone marrow
38 monocytes. CD122+Macs develop in the uterus and placenta with kinetics that mirror interferon
39 (IFN) activity at the maternal-fetal interface. Macrophage colony-stimulating factor (M-CSF)
40 permits macrophages to express CD122, and IFNs are sufficient to drive expression of CD122 on
41 macrophages. Neither Type-I nor Type-II IFNs are required to generate CD122+Macs, however.
42 In response to IL-15, CD122+Macs activate the ERK signaling cascade and enhance production
43 of proinflammatory cytokines after stimulation with the Toll-like receptor 9 agonist CpG. Finally,
44 we provide evidence of human cells that phenocopy murine CD122+Macs in secretory phase
45 endometrium during the implantation window and in first-trimester uterine decidua. Our data
46 support a model wherein IFNs local to the maternal-fetal interface direct novel IL-15-responsive
47 macrophages with the potential to mediate IL-15 signals critical for optimal outcomes of
48 pregnancy.

49 INTRODUCTION

50 The notion of immune quiescence during pregnancy forms the basis for the decades-old central
51 tenet of reproductive immunology (1). However, countless pieces of evidence now support that
52 the action of proinflammatory cytokines are critical to a healthy gestation for both mother and
53 fetus (2). As in many other contexts, though, the proinflammatory response must be regulated in
54 order to avoid an adverse outcome of pregnancy caused by damage to the developing fetoplacental
55 unit.

56
57 Perturbation in homeostasis of the pleiotropic cytokine interleukin-15 (IL-15) has been linked to
58 poor maternal and fetal outcomes of pregnancy in mice and humans. Mice lacking IL-15 (*Il15^{-/-}*)
59 bear growth-restricted pups and exhibit higher rates of spontaneous resorptions than do IL-15-
60 sufficient mice (3, 4). Mice deficient in either production of IL-15 or responsivity to IL-15 exhibit
61 abnormal utero-placental anatomy, including impaired remodeling of the uterine spiral arteries, a
62 pathologic hallmark of life-threatening preeclampsia in humans (5). These data translate well to
63 findings of reduced IL-15 in human placentae of pregnancies affected by preeclampsia (6).
64 Conversely, IL-15 permits inflammatory-mediated fetal loss in mice (4). Indeed, spontaneous and
65 recurrent miscarriage in humans is associated with unrestrained expression of IL-15 mRNA and
66 protein (7).

67
68 IL-15 is abundant during normal pregnancy. In mice, IL-15 mRNA is expressed in the non-
69 pregnant uterus, as well as in the utero-placental unit throughout pregnancy, with a peak at mid-
70 gestation (8). In humans, IL-15 mRNA is found in low abundance in proliferative phase
71 endometrium and increases substantially in secretory phase endometrium and first trimester

72 decidua (9). IL-15 protein has been demonstrated in endometrial stromal cells, perivascular cells
73 abutting uterine spiral arteries, and vascular endothelial cells, echoing the presumed roles for IL-
74 15-responsive cells in vascular remodeling.

75

76 In the current model of IL-15 signaling, IL-15 is complexed with the high-affinity α subunit of the
77 IL-15 receptor (IL-15R α) (10). Myeloid cells and non-hematopoietic cells then present the IL-
78 15/IL-15R α complex in trans to IL-15-responsive cells, typically killer lymphocytes bearing high
79 levels of the β chain of the IL-15 receptor complex (CD122) and the common γ chain (γ_c). Indeed,
80 at the maternal-fetal interface, IL-15 is bound to the cell surface of CD14⁺ monocytes and
81 macrophages in single cell suspensions of human first-trimester uterine decidua (9), the uterine
82 lining remodeled to accept an embryo. Consistent with these human data, pregnant mice lacking
83 γ_c but reconstituted with bone marrow from *Il15*^{-/-} mice exhibit normal uterine vascular
84 remodeling. These findings support that the dominant sources of IL-15 in mice also are non-
85 hematopoietic cells and chemo-resistant myeloid cells (11).

86

87 Altogether, these data show that appropriate signaling by IL-15 is critically important to healthy
88 pregnancy. However, the targets and mechanisms of IL-15 signaling at the maternal-fetal interface
89 are incompletely understood. NK cells are the prototypical IL-15-responsive cell type at the
90 maternal-fetal interface. They are highly prevalent in the uterus and produce proinflammatory
91 interferon γ , without which uterine arteries do not remodel and preeclampsia develops in mice
92 (12). Because uterine and other NK cells clearly depend on IL-15 for development (3, 13), it has
93 been presumed that NK cells are responsible for all abnormalities of pregnancy associated with
94 disrupted homeostasis of IL-15.

95
96 We now report that novel macrophages, termed CD122+Macs, express high levels of CD122 in
97 the uterus of mice and humans. Macrophage colony-stimulating factor (M-CSF) permits Type-I
98 and -II interferons to drive expression of CD122 on these macrophages. CD122+Macs respond to
99 IL-15 by activating the ERK signaling cascade, and CD122+Macs stimulated with the Toll-like
100 receptor agonist CpG enhance production of pro-inflammatory cytokines in response to IL-15.
101 CD122+Macs represent a new and unexpected target of IL-15 in the utero-placental unit and, thus,
102 may have significant clinical implications in healthy and complicated pregnancies.

103 **METHODS**

104

105 *Preparation of single-cell suspensions.* Organs of interest were grossly dissected, weighed,
106 minced finely with scissors, and digested in medium containing Liberase TM (Roche) at a final
107 concentration of 0.28WU/mL and DNase (Roche) at a final concentration 30µg/mL for 30 min at
108 37°C with intermittent agitation. Cells were passed through a 70µm filter, and red blood cells
109 were lysed with ACK lysis buffer. Cells were again filtered and counted with a Countess
110 hemocytometer (Thermo Fisher Scientific) prior to proceeding to antibody staining for flow
111 cytometry or cell sorting.

112

113 *Flow cytometry and cell sorting.* Flow cytometry was performed on either a MacsQuant Analyzer
114 10 (Miltenyi), an LSRFortessa (BD), or a CytoFLEX LX (Beckman Coulter). Cell sorting was
115 performed on either a FACS Aria Fusion (BD) or a MoFlo Astrios EQ (Beckman Coulter). Data
116 were exported as FCS files and analyzed using FlowJo 10 software. All antibody staining was
117 performed at 4°C in the dark. Prior to fluorescent antibody staining, cells were incubated with
118 mouse Fc block (TruStain FcX, Biolegend) or human Fc block (BD). Fixable, fluorescent
119 LIVE/DEAD viability dye (Thermo Fisher) was used in Blue, Aqua, Green, and Near-IR per
120 manufacturer recommendations. All antibodies, clones, and concentrations used for flow
121 cytometry and cell sorting are listed in Supplemental Table 3.

122

123 *Microarray.* Sorted cells were pelleted, removed of medium, snap-frozen on dry ice, and stored
124 at -80°C. RNA was isolated using a Micro RNeasy mini total RNA kit (Qiagen), performed
125 according to the manufacturer's instructions. MouseGene 1.0ST chips were used. Microarray data
126 were normalized by the Robust Multichip Average (RMA) algorithm and log₂ transformed using

127 the oligo package in R (14). Linear modeling to obtain differentially expressed genes was
128 performed with the limma package in R (15). A gene was considered significantly differentially
129 expressed with a FDR-adjusted p value less than 0.05. Gene ontology (GO) analysis was
130 performed using DAVID (16, 17).

131

132 *Adoptive transfers.* Single-cell suspensions of bulk bone marrow (BM) were obtained from pooled
133 femorae, tibiae, and humeri of donor mice. Red blood cells were lysed with ACK lysis buffer, and
134 cells were filtered through a 70 μ m filter. Monocytes were enriched with a mouse BM monocyte
135 isolation kit (Miltenyi) by magnetic bead-mediated depletion of non-monocytes. Manufacturer
136 instructions were followed exactly. Purity of transferred BM monocytes was routinely ~90% prior
137 to adoptive transfer.

138

139 *Bone marrow-derived macrophages (BMDMs).* Single-cell suspensions of BM were prepared as
140 above. Adherent cells were removed by incubating bulk bone marrow cells on tissue culture-
141 treated plates for at least 2 hours in complete DMEM (cDMEM, 10% FBS, 1%
142 Pencillin/Streptomycin/Glutamine). Non-adherent cells were then collected, counted, and plated
143 at 5x10⁵ cells/mL in cDMEM containing 10% L929 cell-conditioned medium (LCM, made in our
144 laboratory) for 5-7 days. GM-BMDMs were generated by culturing non-adherent BM cells in
145 cDMEM supplemented with 50ng/mL GM-CSF (Peprotech). CD122+BMDMs were generated
146 by adding 1ng/mL IFN α (Biolegend) to the medium on day 5 of culture. When testing ability of
147 IFN γ (Peprotech) to derive CD122+Macs, doses indicated were added on day 5 of culture. Anti-
148 IFNAR and anti-IFNGR (both BioXcell) were both used at 10 μ g/mL in culture.

149

150 *ELISA.* CD122+BMDMs were generated as above. Cells were washed on day 6 of culture, and
151 medium was replaced with DMEM containing 3% serum for the final 16 hours of culture with or
152 without 1 μ g/mL CpG 1826 (IDT), as indicated. To this medium, IL-15R α alone (IL-15R α Fc
153 chimera protein, R&D Systems) or IL-15R α pre-complexed with IL-15 (Peprotech) was added, as
154 indicated. Final concentrations of IL-15R α and IL-15 were 100ng/mL and 50ng/mL, respectively.
155 Complexing of IL-15R α with IL-15 was performed in PBS at 37°C for 30 minutes. OptEIA
156 ELISA kits (BD) for mouse were used: IL-6 and TNF. Manufacturer instructions were followed
157 precisely, and concentrations of cytokines were determined with a SpectraMax ELISA plate
158 reader.

159

160 *Western blots.* CD122+BMDMs were generated as above. Cells were washed on day 6 of culture,
161 and medium was replaced with serum-free DMEM for 2 hours. Medium was replaced with
162 cDMEM containing IL-15R α alone or IL-15R α /IL-15 complex, as above, for 20 minutes. Whole-
163 cell lysates were then prepared by washing cells in cold PBS and lysing in M-PER Mammalian
164 Protein Extraction Reagent (Thermo Scientific) with protease/phosphatase inhibitor cocktail (Cell
165 Signaling Technology). Lysates were quantified by Bradford assay, normalized, reduced, and
166 resolved by SDS gel electrophoresis on 10% Bis-Tris gels (Invitrogen). Resolved proteins were
167 transferred to 0.45 μ m Nitrocellulose membranes (Bio-Rad). Membranes were blocked in
168 Odyssey Blocking Buffer (Licor) and probed with the following antibodies: pERK (Cell Signaling
169 Technology, 1:1000), total ERK (Cell Signaling Technology, 1:1000), and GAPDH (Novus Bio,
170 1:2000). Membranes were incubated with the following secondary antibodies at a dilution of
171 1:20,000: Alexa Fluor 680 donkey anti-rabbit IgG (Invitrogen) or Alexa Fluor Plus 800 donkey
172 anti-mouse IgG (Invitrogen). Proteins were detected and quantified using a LICOR Odyssey.

173

174 *Human endometrial samples.* Endometrial biopsies were obtained from patients and volunteers at
175 Penn Fertility Care. MAM has approval for the collection endometrial tissue (IRB# 826813).
176 Written informed consent was obtained from all subjects. All women were between the ages of
177 18 and 43, with no significant medical history and regular menstrual cycles (between 25-35 days
178 over the past 3 months). Endometrial biopsies were obtained from known fertile women 8 days
179 after an LH surge (secretory phase), which was detected in the urine by the Clearblue Ovulation
180 Test. All biopsies were obtained using a Pipelle Endometrial Suction Curette (Cooper Surgical).
181 All biopsies were dissociated and analyzed within 24 hours of collection. Single cell suspensions
182 were obtained as above.

183

184 *First trimester decidual tissue.* First trimester decidual tissue was obtained from the Penn Family
185 Planning and Pregnancy Loss center. MAM has IRB approval for the collection of first trimester
186 extraembryonic tissue (IRB# 827072). Written informed consent was obtained from all subjects.
187 After tissue collection, decidua was manually separated from chorionic villi based on gross
188 morphology. All samples were dissociated and analyzed within 24 hours of collection. Single cell
189 suspensions were obtained as above.

190

191 *Statistics.* For non-microarray data, statistical analyses were performed using GraphPad Prism 8.
192 A 1-way ANOVA with a test for linear trend was used to determine whether the slope of a line
193 was likely to have occurred by chance alone. A (non-parametric) Wilcoxon matched-pairs signed
194 rank test was used to compare effect of IL-15 treatment on matched samples. Mixed-effects
195 analysis was used to compare paired observations with one-way ANOVA. Holm-Sidak's multiple

196 comparisons test was used in mixed-effects analyses. In all cases, $P < 0.05$ was considered
197 significant.

198

199 *Mice.* All animals were housed, cared for, and euthanized in accordance with a protocol approved
200 by the Institutional Animal Care and Use Committee (IACUC) of Children's Hospital of
201 Philadelphia. Wild-type mice were strain C57Bl/6, and all knockout mice were on a C57Bl/6
202 background. *Ifnar*^{-/-}, *Ifngr*^{-/-}, and *Ifnar*^{-/-}*Ifngr*^{-/-} mice, LysM-Cre and DTR-mCherry transgenic
203 mice intercrossed to yield MM-DTR mice, and CD45.1 mice were all purchased from The Jackson
204 Laboratory. All animals used were between 6-12 weeks of age. While it was only possible to use
205 female mice to investigate uterine immune cells, both male and female mice were used for *in vitro*
206 experiments, yielding similar results. For pregnant female mice, presence of copulation plugs were
207 checked early each morning. Copulation was assumed to take place during the 12-hour dark cycle
208 (from 6PM-6AM in our facility). Thus, E0.5 denotes the morning that a copulation plug was first
209 detected.

210

211 RESULTS

212 *CD122+ macrophages are enriched in the uterus in mice*

213 To determine whether uterine leukocytes other than NK cells could be cellular targets of IL-15,
214 we comprehensively examined expression of CD122 on immune cells in pregnant female mice.
215 Populations of cells co-expressing CD122 and high levels of macrophage/monocyte-associated Fc
216 γ Receptor 1 (Fc γ RI, CD64) and F4/80 were evident in several organs but were particularly
217 enriched in the uterus of pregnant and non-pregnant mice (Fig. 1A, Supplemental Fig. 1A). Other
218 myeloid-phenotype cells, such as Ly6G⁺ cells (neutrophils) and CD11^{cbright}MHCII^{bright} cells
219 (conventional dendritic cells, DCs), did not exhibit surface expression of CD122 (Fig. 1A). During
220 gestation, these CD122⁺ phenotypic macrophages (herein CD122⁺Macs) were present throughout
221 the maternal fetal interface: in the myometrium, mesometrial lymphoid aggregate of pregnancy
222 (MLAP), decidua, and placenta (Fig. 1B).

223

224 Rarely are classical myeloid and lymphoid proteins co-expressed in the same cell. Recently, NK
225 cells expressing canonical myeloid transcripts, including *Csf1r*, were identified in obese mice and
226 humans (18). Thus, it was possible that CD122⁺Macs represented a subpopulation of so-called
227 myeloid NK cells, given the high abundance of NK cells in the early gestation uterus. In order to
228 determine to which lineage uterine CD122⁺Macs cells belonged, we compared their morphology
229 to other uterine cell types. Murine uterine CD122⁺F4/80^{bright} cells were morphologically large and
230 hyper-vacuolated, similar to conventional CD122⁻ macrophages (cMacs, Supplemental Fig. 1B,
231 1C). The cell surface phenotype of CD122⁺Macs overlapped substantially with that of cMacs.
232 Most CD122⁺Macs and cMacs were CD11^{cint}, Ly6C^{low/neg}, CCR2^{hi}, and MERTK^{hi}, a constellation
233 of findings typically associated with macrophages (Fig. 1C, 1D). Aside from CD122,

234 CD122+Macs and cMacs could be distinguished by expression of MHC Class II (MHCII), with
235 CD122+Macs largely MHCII_{low} and cMacs largely MHCII_{hi} (Fig. 1C).

236

237 In contrast to CD122+Macs and cMacs, the morphology and flow cytometric profile of
238 CD122+F4/80-CD64- cells were consistent with classical large, granular, decidual NK cells (Fig.
239 1C, Supplemental Fig. 1B-E). Nearly all decidual NK cells express NKp46 and the tissue-resident
240 NK cell marker CD49a, especially early in gestation (19). We found that CD122+Macs did not
241 express CD49a, CD49b/DX5, T-bet or Eomesodermin (Supplemental Fig. 1E), closely-related
242 master regulators of innate lymphoid fate that are abundantly expressed in uterine innate lymphoid
243 cells (19-21). Morphologic and phenotypic data thus supported the notion that CD122+Macs cells
244 are indeed macrophage-lineage cells and not NK cells, DCs, or neutrophils.

245

246 We next tested whether CD122+Macs were most like macrophages or another cell type at the level
247 of the transcriptome. A monocyte-macrophage-specific reporter system, known as the MM-DTR
248 mouse, fluorescently labels with mCherry monocytes and macrophages that transcribe both *Lyz2*
249 (*LysM*) and *Csf1r* (macrophage colony-stimulating factor receptor, M-CSFR) (22). Expression of
250 CD122 directly correlated with expression of mCherry in F4/80_{bright} cells in the uterus (Fig. 1E).
251 We then sort-purified decidual CD122+Macs, cMacs, and NK cells to a purity of at least 95%
252 (Supplemental Fig. 1F) and analyzed the transcriptome using microarrays. We found that 86.5%
253 of the variance in gene expression among these populations could be attributed to the first principal
254 component, PC1 (Fig. 1F). Clustering samples along PC1 clearly separated cMacs and
255 CD122+Macs from NK cells. Similarly, hierarchical clustering analysis showed that all
256 macrophages were closely related to each other but distantly related to NK cells (Fig. 1G). Among

257 genes enriched in CD122+Macs relative to NK cells were those classically associated with
258 macrophages, including numerous complement receptors, Toll-like receptors, and *Cd68*, *Csf1r*,
259 *Fcgr1*, *Lyz2*, and *Cx3cr1* (Supplemental Table 1). Among genes enriched in NK cells relative to
260 CD122+Macs were those typically associated with innate and killer lymphocytes, including *Ncr1*
261 (NKp46), transcripts encoding cytolytic mediators, Ly49 receptors, and *Eomes* (Eomesodermin)
262 and *Tbx21* (T-bet). Of note, some cytolytic genes, including *Prf1* and several granzymes, were
263 modestly but significantly enriched in CD122+Macs relative to cMacs (Fig. 1H, Supplemental
264 Table 2). Altogether, these data support the notion that CD122+Macs and cMacs are highly related
265 but distinct subtypes of uterine macrophages.

266

267 *CD122+Macs are present in human endometrium and decidua*

268 Given the unusual phenotype and restricted anatomic location of CD122+Macs in mice, we
269 assessed whether such macrophages were also found in the human uterus. We therefore examined
270 human secretory endometrium during the implantation window, as well as human first-trimester
271 decidua, for the presence of human CD122+Macs (hCD122+Macs). We relied on expression of
272 CD14 and CD64 to identify human classical monocytes and macrophages by flow cytometry
273 (Supplemental Fig. 3A). We defined human NK (hNK) cells as CD14-CD56^{bright} (uterine) or
274 CD14-CD56^{dim} (blood). As expected, hNK cells were abundant in the uterus and expressed high
275 levels of CD122.

276

277 We then identified CD14/CD64⁺ cells enriched in the human pre- and post-implantation uterus
278 that expressed CD122 (Fig. 2A-C, Supplemental Fig. 2A-E, Supplemental Fig. 3A-C). These
279 hCD122+Macs varied widely in abundance among individual samples but were present in all first-

280 trimester deciduae tested (Fig. 2A-C, Supplemental Fig. 2A-E). Human CD122+Macs were also
281 present in over half of human secretory phase endometrial biopsies examined during the
282 implantation window (Fig. 2C, Supplemental Fig. 3A-C). We found that hCD122+Macs often
283 expressed CD16 and variably expressed CD11c, as did human conventional macrophages
284 (hcMacs, Fig. 2B and 2C, Supplemental Fig. 2A-E, Supplemental Fig. 3A). Both hCD122+Macs
285 and hcMacs expressed HLA-DR, but in some samples, hCD122+Macs expressed modestly less
286 HLA-DR, similar to our observations of MHCII levels on CD122+Macs and cMacs in the mouse.
287

288 Human CD122+Macs variably expressed CD56 (Fig. 2A-C, Supplemental Fig. 2A-E,
289 Supplemental Fig. 3A-C). CD56 is typically associated with cytotoxic lymphocytes, but it has
290 been found on myeloid cells in certain contexts (23). Consistent with this literature, human
291 CD122+Macs expressing higher levels of CD56 appeared to express the cytolytic molecules
292 Perforin and Granzyme B at the protein level (Fig. 2B, Supplemental Fig. 2B, 2D and 2E,
293 Supplemental Fig. 3A). These data agree with our transcript-level data in mice, showing
294 enrichment of cytolytic mediators in CD122+Macs relative to cMacs (Fig. 1H, Supplemental Table
295 2). Overall, human CD122+Macs bore striking resemblance to murine CD122+Macs, supporting
296 the use of our murine model to obtain mechanistic insights into the biology of this novel uterine
297 macrophage in humans.

298

299 *Mouse CD122+Macs can derive from monocytes*

300 Our morphologic, phenotypic, and transcriptomic data supported that CD122+Macs were
301 macrophages. Myriad embryonic and adult progenitors give rise to macrophages in different
302 tissues (24, 25). Monocytes are recruited in large numbers to the gravid uterus during gestation

303 (26). We thus tested the hypothesis that CD122+Macs could derive from adult bone marrow
304 monocytes. Magnetic bead-purified Ly6C^{hi} monocytes from adult mouse bone marrow of MM-
305 DTR mice were adoptively transferred into pregnant recipients during the peri-implantation period
306 (Fig. 3A and 3B). Recipients were then sacrificed at mid-gestation. We observed tissue-specific
307 differences in phenotype of recovered donor cells with respect to both F4/80 and CD122. Donor
308 cells recovered from recipient blood, spleen, and bone marrow were almost uniformly F4/80^{int}
309 (Fig. 3B), suggesting maintenance of monocyte fate. In contrast, donor cells recovered from
310 recipient peritoneum, myometrium, and decidua contained F4/80^{bright} cells, suggesting some
311 conversion to tissue macrophages in these organs.

312

313 Despite conversion of monocytes to F4/80^{bright} cells in the peritoneum, we found that transferred
314 monocytes converted to macrophages expressing high levels of CD122 only in the uterus (Fig.
315 3B). These data are consistent with our findings that CD122+Macs are enriched in the uterus in
316 the steady state. Of note, we performed this experiment with both pregnant and non-pregnant
317 donors with identical results (data not shown), suggesting no intrinsic differences in potential of
318 bone marrow monocytes between pregnant and non-pregnant mice. Altogether, our data support
319 a model in which bone marrow monocytes are recruited to the uterus and differentiate into
320 CD122+Macs.

321

322 *Tissue-specific population dynamics of CD122+Macs during gestation*

323 Populations of myeloid cells, including dendritic cells, monocytes, and macrophages, are in
324 constant flux at the maternal-fetal interface during gestation (26, 27). We thus investigated
325 population dynamics of uterine CD122+Macs before and during pregnancy in the mouse. The

326 myometrium exhibited progressive percent enrichment of F4/80^{bright} cells over the course of
327 gestation (Fig. 4A and 4B), which agrees with and extends prior findings (26). This was in contrast
328 to progressive declines in NK cells after mid-gestation (Fig. 4A-C), consistent with prior reports
329 (28). On a percentage basis, myometrial CD122+Macs were more apparent over the course of
330 gestation until E16.5 (Fig. 4A and B). By E12.5 and before E16.5, myometrial CD122+Macs also
331 exhibited more robust expression of CD122 on a per-cell basis. The absolute numbers of
332 CD122+Macs per gram of myometrial tissue remained relatively stable through mid-gestation but
333 declined thereafter (Fig. 4C).

334

335 Similar to the myometrium, the combined decidual and placental layers exhibited progressive
336 decline in NK cells but progressive relative enrichment of CD122+Macs during pregnancy (Fig.
337 4A and 4B). Unlike the myometrium, however, this relative enrichment of CD122+Macs in the
338 decidua and placenta appeared to be at the expense of F4/80^{bright} cMacs in those tissue layers. Also
339 unlike the myometrium, a robust proportion and absolute number of CD122+Macs persisted as
340 gestation approached term (Fig. 4B and 4C). In the early post-implantation period through E10.5,
341 CD122+Macs expressed moderate amounts of CD122 in the decidua and placenta (Fig. 4A and
342 4B). From E11.5 through E18.5, the last timepoint we examined before delivery, deciduo-
343 placental CD122+Macs exhibited progressively more robust expression of CD122 on a per-cell
344 basis.

345

346 In the non-pregnant uterus, we observed a population of CD122+F4/80^{int} cells that became less
347 apparent but persisted throughout pregnancy (Fig. 4A and 4B). These cells could have represented
348 monocytes/macrophages or F4/80⁺ uterine eosinophils (29). Our data confirmed that presumptive

349 eosinophils, with high side scatter properties and low to no expression of CD64, are abundant
350 within the bulk F4/80_{int} population (data not shown). However, these cells were uniformly
351 negative for CD122. F4/80_{int}CD122⁺ cells, on the other hand, exhibited lower side scatter
352 properties and were CD64⁺, consistent with monocytes/macrophages. These data reinforce a
353 model in which monocytes and macrophages are the only uterine myeloid cells that express surface
354 CD122. Further, these data provide evidence for a model in which populations of CD122⁺
355 monocytes and macrophages are dynamically regulated in a tissue layer-specific fashion in the
356 pre-pregnant and gravid uterus.

357

358 *Type-I and II interferons are sufficient for development of CD122+Macs*

359 Our data suggested that the uterus strongly favored development of CD122+Macs. Further, the
360 drivers of the CD122+Mac fate appeared transiently strongest just after mid-gestation in the
361 myometrium and persistently strong from mid-gestation through near-term in the deciduo-
362 placental unit. Total interferon (IFN) activity at the mouse maternal-fetal interface precisely
363 mirrors the population dynamics of CD122+Macs (30). The non-pregnant uterus transcribes Type-
364 I IFN and IFN-stimulated genes (ISGs) (31), and Type-II IFN is apparent during the estrous phase
365 (32). In the pregnant myometrium, total IFN activity is low until E10, peaks between E11 and
366 E15, then returns to low levels after E15 (30). IFN activity is already robust in the developing
367 placenta at E10 but spikes dramatically after E10 through to term.

368

369 To understand whether IFNs played a role in development of uterine CD122+Macs, we first
370 compared the transcriptomes of decidual cMacs and CD122+Macs during early gestation, when
371 both cell types were present and in similar abundance. Review of individual transcripts and gene

372 ontology (GO) analysis of transcripts significantly upregulated in CD122+Macs relative to cMacs
373 showed strong enrichment of genes associated with interferon signaling and antiviral responses
374 (Fig. 5A, Supplemental Table 2). With this information, we next sought to determine whether
375 IFNs were sufficient to drive expression of CD122 on decidual macrophages. F4/80+ cells in bulk
376 single-cell suspensions of early gestation decidual capsules exhibited a dose-dependent
377 upregulation of surface CD122 upon exposure to recombinant IFN α , though this effect was
378 strongest in F4/80_{int} cells (Fig. 5B and data not shown). To extend these findings, we cultured
379 sort-purified uterine F4/80_{int} monocytes in macrophage colony-stimulating factor (M-CSF) with
380 or without Type-I IFN α . Consistent with the notion that culture in macrophage colony-stimulating
381 factor (M-CSF) results in endogenous production of Type-I IFN by macrophages (33), we did
382 observe some expression of CD122 on uterine monocytes cultured in M-CSF alone (Fig. 5B and
383 5C). However, addition of IFN α resulted in robust upregulation of CD122+ compared to culture
384 in M-CSF alone.

385
386 Further, we could derive CD122+Macs *in vitro* from nonadherent bone marrow cells. Traditional
387 bone marrow-derived macrophages cultured with M-CSF (BMDMs) upregulated CD122 in a dose-
388 dependent fashion in response to both Type-I IFN α and Type-II IFN γ (Fig. 5D and 5E). While
389 the ability to drive expression of CD122 on BMDMs was shared by both Type-I and II IFNs, we
390 did observe differential effects of Type-I and -II IFNs on expression of MHCII (Supplemental Fig.
391 4A), in agreement with prior reports (34). Consistent with endogenous production of Type-I IFN
392 by M-CSF-stimulated macrophages (33), blockade of the Type-I IFN receptor (IFNAR) nearly
393 abolished expression of CD122 by BMDMs cultured in M-CSF alone (Fig. 5D and 5E). Blockade
394 of the IFN γ receptor (IFNGR), however, had no effect on level of CD122 in BMDMs cultured in

395 M-CSF alone, suggesting that BMDMs do not produce endogenous IFN γ . Use of combined Type-
396 I/Type-II IFN receptor knockout BMDMs (*Ifnar*^{-/-}*Ifngr*^{-/-} double-knockout, DKO) showed that
397 DKO BMDMs appropriately do not upregulate CD122 with IFN treatment (Fig. 5F). However,
398 we detected modest but nonzero levels of CD122 on DKO BMDMs by virtue of culture in M-CSF.
399 Thus, IFNs enhance expression of CD122, but they are not strictly required for expression of
400 CD122 on BMDMs.

401

402 To determine whether expression of CD122 by BMDMs in response to IFNs was a phenomenon
403 universal to all macrophages, we generated “GM-BMDMs” by culturing nonadherent bone
404 marrow in medium supplemented with high-dose granulocyte-macrophage colony-stimulating
405 factor (GM-CSF), instead of M-CSF (35, 36). Consistent with prior reports (35), GM-BMDMs
406 upregulated CD11c and MHCII to a greater extent than traditional BMDMs (Supplemental Fig.
407 4B). Also in contrast to traditional BMDMs, GM-BMDMs produce less endogenous Type-I IFN
408 (36). Indeed, we observed that GM-BMDMs exhibited little to no expression of CD122 relative
409 to traditional BMDMs (Fig. 5F, Supplemental Fig. 4B). While traditional BMDMs upregulated
410 CD122 robustly in response to Type-I IFN, GM-BMDMs did not change expression of CD122 in
411 response to exogenous Type-I IFN. Taken together, these data support a model in which M-CSF
412 primes bone marrow monocytes to develop into macrophages capable of upregulating CD122 in
413 response to IFNs.

414

415 *Type-I and II interferons are not required for development of CD122⁺Macs in vivo*

416 We next assessed whether responsiveness to Type-I and/or II IFNs was required for development of
417 uterine CD122⁺Macs *in vivo*. As CD122⁺Macs could derive from monocytes, we chose to first

418 determine requirements for Type-I and II IFNs in generation of CD122+Macs with adoptive
419 transfer of BM monocytes. While recovery of adoptively transferred cells from mice not treated
420 with radiation or chemotherapy is low, this approach allows for testing of cell-intrinsic
421 requirements for Type-I and -II IFNs in development of uterine CD122+Macs in normal
422 pregnancy. As discussed above, both Type-I and -II IFNs are produced at the maternal-fetal
423 interface (30-32). Recently, Type-III IFN λ was shown to play a critical role in fetal protection
424 against infection with Zika virus in mice and humans (37, 38). Thus, all three known families of
425 IFN are actively produced at the maternal-fetal interface. Combined with our data that either Type-
426 I or -II IFN is sufficient to induce expression of CD122 on BMDMs in vitro, we hypothesized that
427 there would be no specific IFN required for development of CD122+Macs. In other words, any
428 class of IFN might be able to signal to uterine macrophages to differentiate into CD122+Macs.
429 Consistent with this hypothesis, donor-derived CD122+Macs were equally evident after transfer
430 of BM monocytes from wild-type, Type-I IFN receptor-deficient (IFNAR KO), Type-II IFN
431 receptor-deficient (IFNGR KO), and DKO mice (Fig. 6A and 6B). Consistent with these data, we
432 also found similar abundance of uterine CD122+Macs in non-pregnant IFNAR KO, IFNGR KO,
433 and DKO mice (Fig. 6C). Altogether, these data support that receptivity to Type-I and -II IFNs,
434 alone or in combination, is not required for BM monocytes to reach the uterus and develop into
435 CD122+Macs.

436

437 *IL-15 signals through CD122 to enhance function of CD122+Macs*

438 Despite the observed expression of CD122 by CD122+Macs, if and how IL-15 signals to
439 macrophages remained unknown. IL-15 has been shown to signal through CD122 and the
440 common gamma chain (γ_c), which results in phosphorylation of numerous downstream targets,

441 including ERK (39). To test for phosphorylation of ERK in CD122+Macs exposed to IL-15, we
442 first created CD122+BMDMs by culturing nonadherent bone marrow cells in M-CSF plus IFN α .
443 Cytokines already present in culture, including exogenous IFN α , were then removed by washing
444 adherent cells thoroughly and adding fresh, cytokine-free medium. Washed CD122+BMDMs
445 were then stimulated in the presence or absence of IL-15 pre-complexed to the α chain of the IL-
446 15 receptor (IL-15R α), which most closely approximates true presentation of IL-15 *in vivo* and
447 optimizes its activity (40). BMDMs stimulated with IFN express IL-15R α (41), which can
448 transduce IL-15 signals in the absence of CD122 in certain cell types (42). Use of a pre-associated
449 IL-15/IL-15R α complex, rather than free IL-15, ensured that any effects seen by stimulating
450 CD122+BMDMs with IL-15 would be mediated through CD122/ γ_c and not IL-15R α . After 30
451 minutes of stimulation, we observed robust phosphorylation of ERK1/2 in cells treated with the
452 IL-15 complex (Fig. 7A and 7B). These data support that IL-15 signals through CD122 in
453 macrophages using the ERK/MAPK cascade, similar to other IL-15-responsive cell types.

454
455 We next tested whether IL-15 could act on CD122+Macs to modulate production of cytokines.
456 CD122+BMDMs stimulated with the Toll-like receptor 9 (TLR9) agonist CpG produced abundant
457 tumor necrosis factor α (TNF α) and IL-6 (Fig. 7C). Those CD122+BMDMs co-stimulated with
458 CpG and IL-15 pre-complexed to IL-15R α exhibited enhanced production of TNF α and IL-6 (Fig.
459 7C, Supplemental Fig. 7), but we did not observe changes in levels of IL-10 (data not shown).
460 Overall, these data support that CD122+Macs are novel cellular targets for IL-15.

461 **DISCUSSION**

462 Macrophages are critical for successful pregnancy. Severe abnormalities of pregnancy are found
463 in osteopetrotic (*op/op*) mice that lack functional M-CSF and exhibit substantially reduced uterine
464 macrophages (43). Implantation of the embryo is compromised and litter sizes are small relative
465 to M-CSF-sufficient mice. *Op/op* dams cannot be mated with *op/op* sires, as the complete absence
466 of M-CSF is incompatible with gestation of live litters. These data complement a later study
467 showing that inducible deletion of macrophages early in pregnancy causes complete fetal loss,
468 because macrophages sustain the vasculature of ovarian corpus luteum, required to produce
469 progesterone and maintain early pregnancy (29).

470

471 Macrophages are abundant at the maternal-fetal interface and have been shown to directly abut
472 blood vessels and NK cells (44). Fetal trophoblasts of the developing placenta are thought to
473 communicate bidirectionally with macrophages, but few studies have formally addressed this (45,
474 46). These findings suggest that uterine and placental macrophages serve numerous critical
475 functions in pregnancy but are likely heterogenous. Several groups have investigated macrophage
476 heterogeneity during pregnancy in mice and humans (47, 48), but subsets of uterine macrophages
477 remain incompletely described. In this work, we address a critical unmet need to gain a deeper
478 understanding of signals that drive phenotype and function of macrophages at the maternal-fetal
479 interface.

480

481 We found novel and unexpected uterine macrophages that express CD122 and respond to IL-15
482 under direction of M-CSF and IFNs. While IL-2 also signals to cells expressing CD122 and γ_c ,
483 IL-2 is absent from the maternal-fetal interface in the steady state (8). These data suggest that

484 CD122+Macs respond specifically to IL-15 during steady state pregnancy. Gene ontology analysis
485 confirmed that the transcriptome of CD122+Macs is enriched in ISGs. IFNs are classically
486 produced in response to viral infections, but IFNs are abundant in the cycling uterus and at the
487 maternal-fetal interface in the steady state. Type-I and -II IFNs were sufficient to drive expression
488 of CD122 on uterine and bone marrow-derived monocytes and macrophages. However, neither
489 Type-I nor Type-II IFN was required, alone or in combination, to generate CD122+Macs in the
490 uterus of knockout mice or from BM monocytes adoptively transferred into pregnant hosts.
491 Further, M-CSF alone could drive modest expression of CD122 on cultured BMDMs
492 independently of IFN. These data suggest that a combination of factors, likely including some we
493 have yet to investigate, promote development of CD122+Macs in the uterus. We also
494 acknowledge the possibility that Type-III IFN could play a role in shaping the fate of
495 CD122+Macs, though this remains to be tested. Type-III IFN is the most recently described IFN,
496 and extremely limited information is available about its presence at the maternal-fetal interface
497 (38). Like Type-I and -II IFN, Type-III IFN signals through STAT1 and activates networks of
498 canonical ISGs (49, 50). Of note, Type-III IFN appears to activate a network of genes most similar
499 to that of Type-I IFNs (51). Future investigations are needed to address the effects of Type-III
500 IFN on uterine macrophages.

501

502 While both Type-I and Type-II IFNs are capable of directing macrophages to upregulate CD122
503 in vitro, it remains to be determined which IFNs do so in vivo. It is possible that several different
504 interferons at several different timepoints in pregnancy act on macrophages, as observed
505 developmental kinetics of CD122+Macs mirrored that of total IFN activity in the uterus and
506 placenta (30). Mouse and human uterine glandular epithelial cells are an established reservoir of

507 Type-I IFN (52, 53). For example, the Type-I IFN ϵ is produced by uterine epithelium under
508 direction of estrogen (53). While a population of CD122+Macs exists in the non-pregnant uterus
509 of IFNAR KO mice under direction of M-CSF and a non-Type-I IFN and/or additional signal,
510 IFN ϵ may still contribute to development of CD122+Macs in the normal non-pregnant uterus.

511

512 Regulation of IFN γ during murine pregnancy has been thoroughly described (54). Levels
513 progressively rise to a peak at mid-gestation, after which levels halve but plateau to near-term.
514 The cells upon which we performed gene expression profiling were obtained on E7.5, when levels
515 of uterine IFN γ are known to be relatively low. Consistent with those data, gene expression and
516 gene ontology analyses of CD122+Macs appeared most consistent with a Type-I or -III IFN
517 signature. The transcriptome of CD122+Macs was dominated by ISGs, including *Mx1*, that are
518 induced preferentially in response to IFN-I and -III (49, 55). Further, CD122+Macs are largely
519 MHCII_{low} in vivo. Type-II IFN has been shown to enhance expression of MHCII in antigen
520 presenting cells, while IFN-I has been shown to oppose IFN-II-mediated upregulation of MHCII
521 (34). We also showed that treatment of BMDMs with IFN γ in vitro led to upregulation of CD122
522 and MHCII, while treatment of BMDMs with IFN α led to upregulation of CD122 but not MHCII.
523 The IFN system is complex and redundant, particularly the Type-I and Type-III families of IFNs,
524 each composed of several members. This makes isolating individual actors in vivo difficult.
525 Future work will be directed at dissecting this complex system to determine the in vivo IFN
526 requirements for generation of CD122+Macs during pregnancy.

527

528 We observed that only macrophages, not other uterine myeloid cells, express CD122. Further,
529 only CD122+Macs, not CD122+ NK cells, experienced a boost in expression of CD122 on a per-

530 cell basis that correlated with increased IFN activity during gestation. One interpretation is that
531 only macrophages are in close enough proximity to the local source of IFN to express CD122
532 under direction of IFNs. An alternative explanation is that upregulation of CD122 in response to
533 IFN is a mechanism unique to monocytes and macrophages. In support of this latter hypothesis,
534 we provided evidence in vitro that M-CSF-derived macrophages, not GM-CSF-derived
535 macrophages, responded to IFN by upregulating CD122. These data point to unique regulation of
536 *Il2rb* in macrophages, allowing it to be expressed rapidly upon signaling by IFNs. Relatively little
537 is known about transcriptional regulation of *Il2rb* (56, 57), and further investigations into why
538 macrophages uniquely respond to IFN by upregulating CD122 are needed. This is especially true
539 in light of the fact that CD122+Macs express neither Eomes nor T-bet, which have been previously
540 shown to drive expression of *Il2rb* in killer lymphocytes (58). In summary, our data support the
541 notion that CD122 is a novel, macrophage-specific, IFN-stimulated gene.

542

543 Our data show that CD122+Macs can derive from BM monocytes, but the precise precursors of
544 CD122+Macs have yet to be determined. We found evidence of CD122+F4/80_{int} cells in the non-
545 pregnant uterus that likely represent CD122+ monocytes. These cells may represent an
546 intermediate through which CD122+Macs transit during gestation. It has long been appreciated
547 that M-CSF is critical for pregnancy and is positively regulated by sex hormones (43, 59, 60). M-
548 CSF concentrations are at or below the limits of detection in the uterus of non-pregnant mice but
549 increase dramatically in the myometrium during gestation, reaching peak concentration at term
550 (26, 59, 60). Indeed, we showed that large, F4/80_{bright} macrophages were absent from the non-
551 pregnant uterus. The appearance of these cells in the pregnant uterus suggests they may derive
552 from uterine monocytes exposed to M-CSF. In contrast to the myometrium, concentration of M-

553 CSF is modest and constant in the decidua and placenta as gestation progresses (59). Reinforcing
554 these data, additional work showed maintenance of myeloid cells in the growing myometrium and
555 decline of myeloid populations in the decidua as gestation progresses (26, 27). These data are
556 consistent with our observations that adoptively transferred monocytes converted into
557 F4/80^{bright}CD122⁺Macs in the myometrium but not the decidua or placenta late in gestation (data
558 not shown). Altogether, these data are consistent with a model in which BM monocytes are
559 directed to develop into F4/80^{bright} CD122⁺Macs by M-CSF and IFNs.

560

561 Finally, we found that CD122⁺Macs exhibit a biochemical and functional response to stimulation
562 with IL-15. Whether CD122⁺Macs respond to IL-15 in the same manner as classical IL-15-
563 responsive killer lymphocytes, however, remains to be determined. It has long been appreciated
564 that IL-15 enhances cytotoxicity of NK cells (61), and we found it intriguing that CD122⁺Macs
565 expressed a number of cytolytic transcripts. IL-15 may be responsible for the expression of
566 granzymes and perforin observed in CD122⁺Macs, as IL-15 has been implicated in driving
567 expression of cytolytic mediators in human plasma cells (62), another non-traditional responder to
568 IL-15.

569

570 We also have yet to understand the specific stimuli responsible for activating uterine and placental
571 macrophages in vivo during pregnancy, but it is feasible that CD122⁺Macs respond to IL-15 by
572 enhancing production of proinflammatory cytokines that may favor or threaten a healthy
573 pregnancy. For instance, decidual CD122⁺Macs were enriched in *Il18* transcript (encoding IL-
574 18), which is known to support production of IFN γ at the maternal-fetal interface. Establishing
575 this link may have major clinical relevance. Mice deficient in IFN γ signaling fail to remodel

576 uterine spiral arteries into low-resistance, high-capacitance vessels (12). In the mouse, this has
577 been attributed to defective production of IFN γ by NK cells. Further, IL-12 and IL-18 appear to
578 play a key role in production of IFN γ at the maternal fetal interface, as mice deficient in either or
579 both of these cytokines exhibit similarly abnormal uterine artery remodeling as does the IFN γ KO
580 mouse (63). Thus, these mice develop the correlate of human preeclampsia (12, 64). At the same
581 time, hyper-stimulation of CD122+Macs with an over-abundance of IL-15 may contribute to
582 similar adverse outcomes of pregnancy, as seen in a mouse model of spontaneous preeclampsia
583 characterized by an abundance of IL-15 and a relative paucity of NK cells (65). Investigations
584 into the IL-15-dependent and IL-15-independent functions of CD122+Macs in pregnancy are
585 ongoing and may shed light on new therapies for preeclampsia.

586
587 Lending validation to our findings in the mouse, we discovered that the human uterus contains a
588 population of CD122+Macs. We observed that these cells phenocopied mouse CD122+Macs,
589 with expression of CD122 and modest levels of NK cell markers, such as CD56, Perforin, and
590 Granzyme. Human CD122+Macs were not as abundant as mouse CD122+Macs early in gestation,
591 but we have yet to fully explore how this population changes over gestation in humans. We also
592 have yet to formally determine whether these human womb-associated, killer-like macrophages
593 develop, signal, and function like their murine counterparts. A prior report supports the notion
594 that IFNs may be able to drive expression of CD122 in human macrophages, as cultured human
595 blood monocytes can express CD122 after culture in high-dose IFN γ (66). Our findings greatly
596 extend and provide critical context for these prior data. How IFNs signal to human monocytes and
597 macrophages is a key area of ongoing investigation with clear implications for human pregnancy.
598

599 In summary, we have revealed that IFNs act on uterine macrophages to generate an entirely new
600 and unexpected IL-15-responsive cell type at the maternal-fetal interface, the CD122+
601 macrophage. Given the importance of IL-15 in pregnancy, modulation of CD122+Macs may
602 represent a novel therapeutic target to support pregnancies threatened by fetal growth restriction,
603 fetal loss, and preeclampsia.

604 **ACKNOWLEDGMENTS**

605 None.

606 **REFERENCES**

607

608 1. Billington, W. D. 2003. The immunological problem of pregnancy: 50 years with the hope of

609 progress. A tribute to Peter Medawar. *J. Reprod. Immunol.* 60: 1–11.

610 2. Yockey, L. J., and A. Iwasaki. 2018. Interferons and Proinflammatory Cytokines in Pregnancy

611 and Fetal Development. *Immunity* 49: 397–412.

612 3. Barber, E. M., and J. W. Pollard. 2003. The Uterine NK Cell Population Requires IL-15 but

613 These Cells Are Not Required for Pregnancy nor the Resolution of a *Listeria monocytogenes*

614 Infection. *The Journal of Immunology* 171: 37–46.

615 4. Lee, A. J., N. Kandiah, K. Karimi, D. A. Clark, and A. A. Ashkar. 2013. Interleukin-15 is

616 required for maximal lipopolysaccharide-induced abortion. *J Leukoc Biol* 93: 905–912.

617 5. Gathiram, P., and J. Moodley. 2016. Pre-eclampsia: its pathogenesis and pathophysiology.

618 *Cardiovasc J Afr* 27: 71–78.

619 6. Agarwal, R., A. Loganath, A. C. Roy, Y. C. Wong, and S. C. Ng. 2001. Expression profiles of

620 interleukin-15 in early and late gestational human placenta and in pre-eclamptic placenta.

621 *Molecular Human Reproduction* 7: 97–101.

622 7. Toth, B., T. Haufe, C. Scholz, C. Kuhn, K. Friese, M. Karamouti, A. Makrigiannakis, and U.

623 Jeschke. 2010. Placental Interleukin-15 Expression in Recurrent Miscarriage. *Am J Reprod*

624 *Immunol* 64: 402–410.

625 8. Ye, W., L. M. Zheng, J. D. Young, and C. C. Liu. 1996. The involvement of interleukin (IL)-

626 15 in regulating the differentiation of granulated metrial gland cells in mouse pregnant uterus.

627 *Journal of Experimental Medicine* 184: 2405–2410.

628 9. Kitaya, K., J. Yasuda, I. Yagi, Y. Tada, S. Fushiki, and H. Honjo. 2000. IL-15 expression at

629 human endometrium and decidua. *Biology of Reproduction* 63: 683–687.

- 630 10. Dubois, S., J. Mariner, T. A. Waldmann, and Y. Tagaya. 2002. IL-15 α recycles and
631 presents IL-15 In trans to neighboring cells. *Immunity* 17: 537–547.
- 632 11. Větvička, V., M. Bilej, and P. W. Kincade. 1990. Resistance of macrophages to 5-
633 fluorouracil treatment. *Immunopharmacology* 19: 131–138.
- 634 12. Ashkar, A. A., J. P. Di Santo, and B. A. Croy. 2000. Interferon gamma contributes to
635 initiation of uterine vascular modification, decidual integrity, and uterine natural killer cell
636 maturation during normal murine pregnancy. *Journal of Experimental Medicine* 192: 259–270.
- 637 13. Ashkar, A. A., G. P. Black, Q. Wei, H. He, L. Liang, J. R. Head, and B. A. Croy. 2003.
638 Assessment of Requirements for IL-15 and IFN Regulatory Factors in Uterine NK Cell
639 Differentiation and Function During Pregnancy. *The Journal of Immunology* 171: 2937–2944.
- 640 14. Carvalho, B. S., and R. A. Irizarry. 2010. A framework for oligonucleotide microarray
641 preprocessing. *Bioinformatics* 26: 2363–2367.
- 642 15. Ritchie, M. E., B. Phipson, D. Wu, Y. Hu, C. W. Law, W. Shi, and G. K. Smyth. 2015.
643 limma powers differential expression analyses for RNA-sequencing and microarray studies.
644 *Nucleic Acids Res.* 43: e47.
- 645 16. Huang, D. W., B. T. Sherman, and R. A. Lempicki. 2009. Bioinformatics enrichment tools:
646 paths toward the comprehensive functional analysis of large gene lists. *Nucleic Acids Res.* 37: 1–
647 13.
- 648 17. Da Wei Huang, B. T. Sherman, and R. A. Lempicki. 2009. Systematic and integrative
649 analysis of large gene lists using DAVID bioinformatics resources. *Nature Protocols* 4: 44.
- 650 18. Theurich, S., E. Tsaousidou, R. Hanssen, A. M. Lempradl, J. Mauer, K. Timper, K.
651 Schilbach, K. Folz-Donahue, C. Heilinger, V. Sexl, J. A. Pospisilik, F. T. Wunderlich, and J. C.

- 652 Brüning. 2017. IL-6/Stat3-Dependent Induction of a Distinct, Obesity-Associated NK Cell
653 Subpopulation Deteriorates Energy and Glucose Homeostasis. *Cell Metabolism* 26: 171–184.e6.
- 654 19. Fu, B., Y. Zhou, X. Ni, X. Tong, X. Xu, Z. Dong, R. Sun, Z. Tian, and H. Wei. 2017. Natural
655 Killer Cells Promote Fetal Development through the Secretion of Growth-Promoting Factors.
656 *Immunity* 47: 1100–1113.e6.
- 657 20. Gordon, S. M., J. Chaix, L. J. Rupp, J. Wu, S. Madera, J. C. Sun, T. Lindsten, and S. L.
658 Reiner. 2012. The transcription factors T-bet and Eomes control key checkpoints of natural killer
659 cell maturation. *Immunity* 36: 55–67.
- 660 21. Doisne, J.-M., E. Balmas, S. Boulenouar, L. M. Gaynor, J. Kieckbusch, L. Gardner, D. A.
661 Hawkes, C. F. Barbara, A. M. Sharkey, H. J. M. Brady, J. J. Brosens, A. Moffett, and F. Colucci.
662 2015. Composition, Development, and Function of Uterine Innate Lymphoid Cells. *J. Immunol.*
663 195: 3937–3945.
- 664 22. Schreiber, H. A., J. Loschko, R. A. Karssemeijer, A. Escolano, M. M. Meredith, D. Mucida,
665 P. Guermonprez, and M. C. Nussenzweig. 2013. Intestinal monocytes and macrophages are
666 required for T cell polarization in response to *Citrobacter rodentium*. *J. Exp. Med.* 210: 2025–
667 2039.
- 668 23. Van Acker, H. H., A. Capsomidis, E. L. Smits, and V. F. Van Tendeloo. 2017. CD56 in the
669 Immune System: More Than a Marker for Cytotoxicity? *Front Immunol* 8: 892.
- 670 24. Perdiguero, E. G., and F. Geissmann. 2016. The development and maintenance of resident
671 macrophages. *Nat. Immunol.* 17: 2–8.
- 672 25. Ginhoux, F., and M. Guilliams. 2016. Tissue-Resident Macrophage Ontogeny and
673 Homeostasis. *Immunity* 44: 439–449.

- 674 26. Tagliani, E., C. Shi, P. Nancy, C.-S. Tay, E. G. Pamer, and A. Erlebacher. 2011. Coordinate
675 regulation of tissue macrophage and dendritic cell population dynamics by CSF-1. *J. Exp. Med.*
676 208: 1901–1916.
- 677 27. Collins, M. K., C.-S. Tay, and A. Erlebacher. 2009. Dendritic cell entrapment within the
678 pregnant uterus inhibits immune surveillance of the maternal/fetal interface in mice. *J. Clin.*
679 *Invest.* 119: 2062–2073.
- 680 28. Wang, C., T. Tanaka, H. Nakamura, N. Umesaki, K. Hirai, O. Ishiko, S. Ogita, and K.
681 Kaneda. 2003. Granulated metrial gland cells in the murine uterus: localization, kinetics, and the
682 functional role in angiogenesis during pregnancy. *Microsc. Res. Tech.* 60: 420–429.
- 683 29. Care, A. S., K. R. Diener, M. J. Jasper, H. M. Brown, W. V. Ingman, and S. A. Robertson.
684 2013. Macrophages regulate corpus luteum development during embryo implantation in mice. *J.*
685 *Clin. Invest.* 123: 3472–3487.
- 686 30. Fowler, A. K., C. D. Reed, and D. J. Giron. 1980. Identification of an interferon in murine
687 placentas. *Nature* 286: 266–267.
- 688 31. Hermant, P., C. Francius, F. Clotman, and T. Michiels. 2013. IFN- ϵ is constitutively
689 expressed by cells of the reproductive tract and is inefficiently secreted by fibroblasts and cell
690 lines. *PLoS ONE* 8: e71320.
- 691 32. Platt, J. S., and J. S. Hunt. 1998. Interferon-gamma gene expression in cycling and pregnant
692 mouse uterus: temporal aspects and cellular localization. *J Leukoc Biol* 64: 393–400.
- 693 33. Moore, R. N., H. S. Larsen, D. W. Horohov, and B. T. Rouse. 1984. Endogenous regulation
694 of macrophage proliferative expansion by colony-stimulating factor-induced interferon. *Science*
695 223: 178–181.

- 696 34. Lu, H. T., J. L. Riley, G. T. Babcock, M. Huston, G. R. Stark, J. M. Boss, and R. M.
697 Ransohoff. 1995. Interferon (IFN) beta acts downstream of IFN-gamma-induced class II
698 transactivator messenger RNA accumulation to block major histocompatibility complex class II
699 gene expression and requires the 48-kD DNA-binding protein, ISGF3-gamma. *Journal of*
700 *Experimental Medicine* 182: 1517–1525.
- 701 35. Lari, R., A. J. Fleetwood, P. D. Kitchener, A. D. Cook, D. Pavasovic, P. J. Hertzog, and J. A.
702 Hamilton. 2007. Macrophage lineage phenotypes and osteoclastogenesis--complexity in the
703 control by GM-CSF and TGF-beta. *Bone* 40: 323–336.
- 704 36. Fleetwood, A. J., H. Dinh, A. D. Cook, P. J. Hertzog, and J. A. Hamilton. 2009. GM-CSF-
705 and M-CSF-dependent macrophage phenotypes display differential dependence on type I
706 interferon signaling. *J Leukoc Biol* 86: 411–421.
- 707 37. Bayer, A., N. J. Lennemann, Y. Ouyang, J. C. Bramley, S. Morosky, E. T. D. A. Marques, S.
708 Cherry, Y. Sadovsky, and C. B. Coyne. 2016. Type III Interferons Produced by Human Placental
709 Trophoblasts Confer Protection against Zika Virus Infection. *Cell Host and Microbe* 19: 705–
710 712.
- 711 38. Jagger, B. W., J. J. Miner, B. Cao, N. Arora, A. M. Smith, A. Kovacs, I. U. Mysorekar, C. B.
712 Coyne, and M. S. Diamond. 2017. Gestational Stage and IFN- λ Signaling Regulate ZIKV
713 Infection In Utero. *Cell Host and Microbe* 22: 366–376.e3.
- 714 39. Adunyah, S. E., B. J. Wheeler, and R. S. Cooper. 1997. Evidence for the involvement of
715 LCK and MAP kinase (ERK-1) in the signal transduction mechanism of interleukin-15.
716 *Biochem. Biophys. Res. Commun.* 232: 754–758.

- 717 40. Rubinstein, M. P., M. Kovar, J. F. Purton, J.-H. Cho, O. Boyman, C. D. Surh, and J. Sprent.
718 2006. Converting IL-15 to a superagonist by binding to soluble IL-15R{alpha}. *PNAS* 103:
719 9166–9171.
- 720 41. Colpitts, S. L., S. W. Stonier, T. A. Stoklasek, S. H. Root, H. L. Aguila, K. S. Schluns, and L.
721 Lefrancois. 2013. Transcriptional Regulation of IL-15 Expression during Hematopoiesis. *The*
722 *Journal of Immunology* 191: 3017–3024.
- 723 42. Marra, P., S. Mathew, A. Grigoriadis, Y. Wu, F. Kyle-Cezar, J. Watkins, M. Rashid, E. De
724 Rinaldis, S. Hessey, P. Gazinska, A. Hayday, and A. Tutt. 2014. IL15RA drives antagonistic
725 mechanisms of cancer development and immune control in lymphocyte-enriched triple-negative
726 breast cancers. *Cancer Research* 74: 4908–4921.
- 727 43. Pollard, J. W., J. S. Hunt, W. Wiktor-Jedrzejczak, and E. R. Stanley. 1991. A pregnancy
728 defect in the osteopetrotic (op/op) mouse demonstrates the requirement for CSF-1 in female
729 fertility. *Developmental Biology* 148: 273–283.
- 730 44. Erlebacher, A. 2013. Immunology of the maternal-fetal interface. *Annu. Rev. Immunol.* 31:
731 387–411.
- 732 45. Fest, S., P. B. Aldo, V. M. Abrahams, I. Visintin, A. Alvero, R. Chen, S. L. Chavez, R.
733 Romero, and G. Mor. 2007. Trophoblast-macrophage interactions: a regulatory network for the
734 protection of pregnancy. *Am J Reprod Immunol* 57: 55–66.
- 735 46. Fock, V., M. Mairhofer, G. R. Otti, U. Hiden, A. Spittler, H. Zeisler, C. Fiala, M. Knöfler,
736 and J. Pollheimer. 2013. Macrophage-derived IL-33 is a critical factor for placental growth. *J.*
737 *Immunol.* 191: 3734–3743.
- 738 47. Houser, B. L., T. Tilburgs, J. Hill, M. L. Nicotra, and J. L. Strominger. 2011. Two unique
739 human decidual macrophage populations. *J. Immunol.* 186: 2633–2642.

- 740 48. Zhao, H., F. Kalish, S. Schulz, Y. Yang, R. J. Wong, and D. K. Stevenson. 2015. Unique
741 roles of infiltrating myeloid cells in the murine uterus during early to midpregnancy. *J. Immunol.*
742 194: 3713–3722.
- 743 49. Kotenko, S. V., G. Gallagher, V. V. Baurin, A. Lewis-Antes, M. Shen, N. K. Shah, J. A.
744 Langer, F. Sheikh, H. Dickensheets, and R. P. Donnelly. 2003. IFN- λ s mediate antiviral
745 protection through a distinct class II cytokine receptor complex. *Nat. Immunol.* 4: 69.
- 746 50. Dickensheets, H., F. Sheikh, O. Park, B. Gao, and R. P. Donnelly. 2013. Interferon-lambda
747 (IFN- λ) induces signal transduction and gene expression in human hepatocytes, but not in
748 lymphocytes or monocytes. *J Leukoc Biol* 93: 377–385.
- 749 51. Donnelly, R. P., and S. V. Kotenko. 2010. Interferon-lambda: a new addition to an old
750 family. *J. Interferon Cytokine Res.* 30: 555–564.
- 751 52. Bulmer, J. N., L. Morrison, P. M. Johnson, and A. Meager. 1990. Immunohistochemical
752 localization of interferons in human placental tissues in normal, ectopic, and molar pregnancy.
753 *Am J Reprod Immunol* 22: 109–116.
- 754 53. Fung, K. Y., N. E. Mangan, H. Cumming, J. C. Horvat, J. R. Mayall, S. A. Stifter, N. De
755 Weerd, L. C. Roisman, J. Rossjohn, S. A. Robertson, J. E. Schjenken, B. Parker, C. E. Gargett,
756 H. P. T. Nguyen, D. J. Carr, P. M. Hansbro, and P. J. Hertzog. 2013. Interferon- ϵ protects the
757 female reproductive tract from viral and bacterial infection. *Science* 339: 1088–1092.
- 758 54. Ashkar, A. A., and B. A. Croy. 1999. Interferon-gamma contributes to the normalcy of
759 murine pregnancy. *Biology of Reproduction* 61: 493–502.
- 760 55. Aebi, M., J. Föh, N. Hurt, C. E. Samuel, D. Thomis, L. Bazzigher, J. Pavlovic, O. Haller, and
761 P. Staeheli. 1989. cDNA structures and regulation of two interferon-induced human Mx proteins.
762 *Molecular and Cellular Biology* 9: 5062–5072.

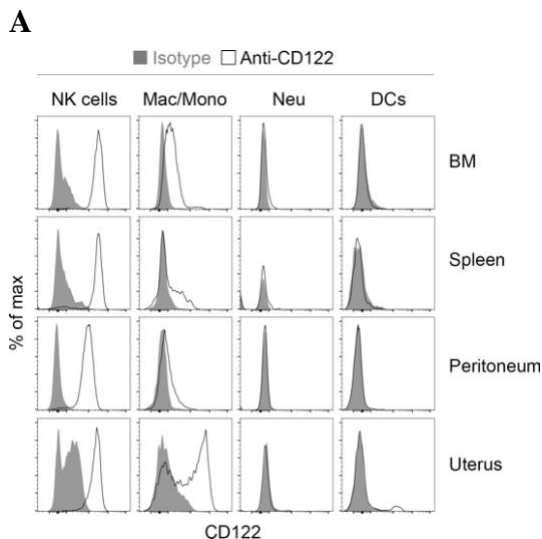
- 763 56. Ye, S.-K., T. J. Kim, S. S. Won, T. J. Yoon, T. K. Park, Y. C. Yoo, Y.-N. Kim, H. C. Lee, K.
764 Ikuta, M.-H. Chung, and K. H. Lee. 2005. Transcriptional regulation of the mouse interleukin-2
765 receptor beta chain gene by Ets and Egr-1. *Biochem. Biophys. Res. Commun.* 329: 1094–1101.
- 766 57. Ohno, S.-I., T. Sato, K. Kohu, K. Takeda, K. Okumura, M. Satake, and S. Habu. 2007. Runx
767 proteins are involved in regulation of CD122, Ly49 family and IFN- γ expression during NK cell
768 differentiation. *Int. Immunol.* 20: 71–79.
- 769 58. Intlekofer, A. M., N. Takemoto, E. J. Wherry, S. A. Longworth, J. T. Northrup, V. R.
770 Palanivel, A. C. Mullen, C. R. Gasink, S. M. Kaech, J. D. Miller, L. Gapin, K. Ryan, A. P. Russ,
771 T. Lindsten, J. S. Orange, A. W. Goldrath, R. Ahmed, and S. L. Reiner. 2005. Effector and
772 memory CD8+ T cell fate coupled by T-bet and eomesodermin. *Nat. Immunol.* 6: 1236–1244.
- 773 59. Bartocci, A., J. W. Pollard, and E. R. Stanley. 1986. Regulation of colony-stimulating factor
774 1 during pregnancy. *Journal of Experimental Medicine* 164: 956–961.
- 775 60. Pollard, J. W., A. Bartocci, R. Arceci, A. Orlofsky, M. B. Ladner, and E. R. Stanley. 1987.
776 Apparent role of the macrophage growth factor, CSF-1, in placental development. *Nature* 330:
777 484–486.
- 778 61. Carson, W. E., J. G. Giri, M. J. Lindemann, M. L. Linett, M. Ahdieh, R. Paxton, D.
779 Anderson, J. Eisenmann, K. Grabstein, and M. A. Caligiuri. 1994. Interleukin (IL) 15 is a novel
780 cytokine that activates human natural killer cells via components of the IL-2 receptor. *Journal of*
781 *Experimental Medicine* 180: 1395–1403.
- 782 62. Xu, W., P. Narayanan, N. Kang, S. Clayton, Y. Ohne, P. Shi, M.-C. Herve, R. Balderas, C.
783 Picard, J.-L. Casanova, J.-P. Gorvel, S. Oh, V. Pascual, and J. Banchereau. 2013. Human plasma
784 cells express granzyme B. *Eur. J. Immunol.* 44: 275–284.

- 785 63. Zhang, J. H., H. He, A. M. Borzychowski, K. Takeda, S. Akira, and B. A. Croy. 2003.
786 Analysis of Cytokine Regulators Inducing Interferon Production by Mouse Uterine Natural
787 Killer Cells1. *Biology of Reproduction* 69: 404–411.
- 788 64. Zhang, J., M. A. Adams, and B. A. Croy. 2011. Alterations in maternal and fetal heart
789 functions accompany failed spiral arterial remodeling in pregnant mice. *American Journal of*
790 *Obstetrics and Gynecology* 205: 485.e1–485.e16.
- 791 65. Sones, J. L., J. Cha, A. K. Woods, A. Bartos, C. Y. Heyward, H. E. Lob, C. E. Isroff, S. D.
792 Butler, S. E. Shapiro, S. K. Dey, and R. L. Davisson. 2016. Decidual Cox2 inhibition improves
793 fetal and maternal outcomes in a preeclampsia-like mouse model. *JCI Insight* 1: 337–17.
- 794 66. Espinoza-Delgado, I., J. R. Ortaldo, R. Winkler-Pickett, K. Sugamura, L. Varesio, and D. L.
795 Longo. 1990. Expression and role of p75 interleukin 2 receptor on human monocytes. *Journal of*
796 *Experimental Medicine* 171: 1821–1826.
- 797
- 798

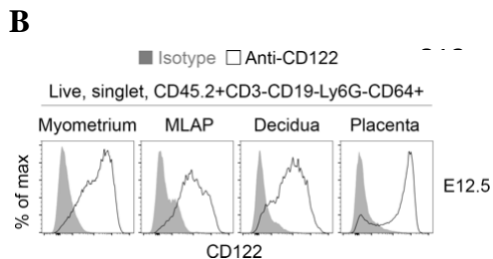
799 **FIGURES AND FIGURE LEGENDS**

800 **FIGURE 1**

801
802



812



819

820

821

822

823

824

825

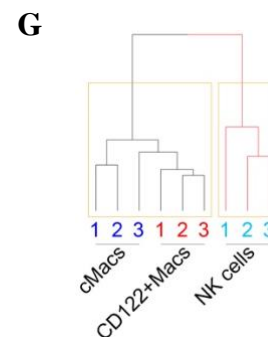
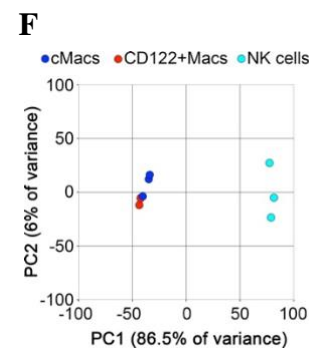
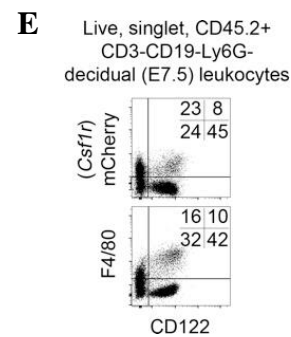
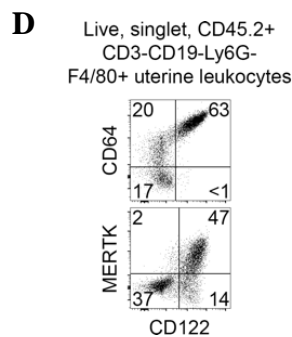
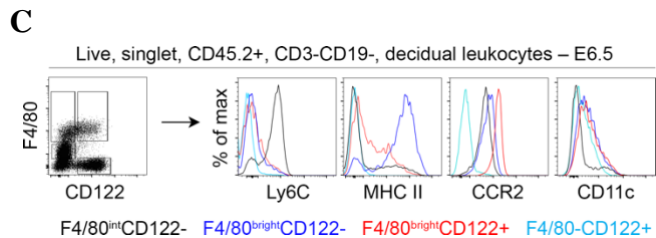
826

827

828

829

830



H

CD122+		Gene	FC
Macs	cMacs		
■	■	<i>Gzma</i>	2.2
■	■	<i>Gzmb</i>	2.4
■	■	<i>Gzmc</i>	2.4
■	■	<i>Gzmd</i>	2.3
■	■	<i>Prf1</i>	2.2

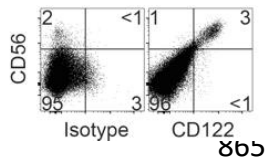
831 **Figure 1. Macrophages expressing CD122 are evident in several organs but are enriched in**
832 **the uterus.** (A) Strong expression of CD122 is evident on macrophage-lineage cells but not other
833 myeloid cells in the bone marrow and uterus. Shaded grey histograms represent isotype control
834 antibody staining, while open histograms show staining with anti-CD122. Indicated populations
835 are gated on live, singlet, CD45.2+ CD3-CD19- leukocytes in non-pregnant mice. “NK cells” are
836 Ly6G-CD64-NKp46+, macrophages and monocytes (“Mac/Mono”) are Ly6G-CD64+NKp46-,
837 neutrophils (“Neu”) are Ly6G+CD64-, and dendritic cells (“DCs”) are Ly6G-CD64-NKp46-
838 CD11c+. Data are representative of at least 10 mice over at least 3 independent experiments. (B)
839 At midgestation in pregnant mice, CD122+Macs are evident in all layers of the maternal-fetal
840 interface. Data are representative of 3 independent experiments with 2-3 mice per experiment.
841 (C) Phenotypically, CD122+F4/80^{bright} cells are macrophage-like but express less MHC Class II
842 and more CCR2 than CD122-F4/80^{bright} cells. Data are representative of at least 5 independent
843 experiments with 2-3 mice per experiment. (D) Uterine CD122+Macs from non-pregnant mice
844 are largely CD64+ and MERTK+. Data are representative of at least 2 independent experiments
845 with 4 total mice. (E) Co-expression of *Lyz2* (LysM) and *Csf1r* (M-CSFR) in CD122+Macs. In
846 “MM-DTR” mice, LysM-Cre acts on a transgene containing *Csf1r* promoter elements, followed
847 by a floxed STOP cassette, followed by an mCherry-Diphtheria toxin receptor fusion protein to
848 specifically label macrophages. Data are representative of at least 5 independent experiments,
849 with at least 2 mice per experiment. (F, G) Transcriptionally, CD122+Macs cluster with CD122-
850 conventional macrophages (cMacs) by (F) principal component analysis (PCA) and (G)
851 hierarchical clustering analysis (HCA). Macs cluster away from NK cells (CD122+F4/80-). Prior
852 to PCA and HCA, control probes and low-variance probes in microarray data were filtered out.
853 Indicated cells were FACS-sorted from 3 independent groups of pooled E7.5 deciduae, with each
854 group consisting of 4-5 mice. (H) Heat map depicting CD122+Macs are enriched in cytolytic
855 transcripts relative to cMacs.
856

857 **FIGURE 2**

858

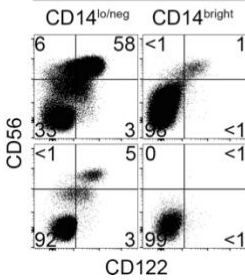
859 **A**

Live, singlet, CD45+CD3-CD19-
CD64+ decidual leukocytes

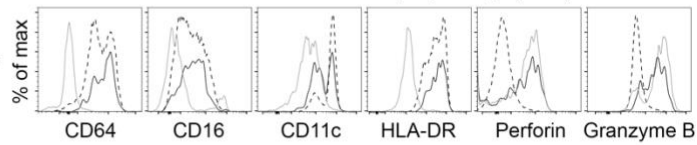


866 **B**

Live, singlet, CD45+
CD3-CD19-leukocytes



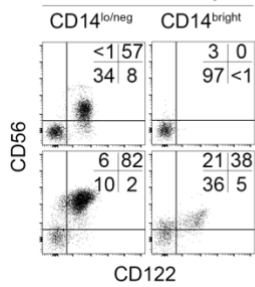
CD14^{br}CD56^{lo}CD122- (cMacs, dashed line)
CD14^{br}CD56^{br}CD122+ (CD122+Macs, solid black line)
CD14^{lo}CD56^{br}CD122+ (NK, solid grey line)



876

877 **C**

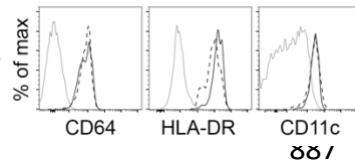
Live, singlet, CD45+
CD3-CD19-leukocytes



Blood

Endo

(cMacs, dashed line)
(CD122+Macs, solid black line)
(NK, solid grey line)



888

889

890 **Figure 2. Human CD122+Macs are evident in the decidua before and during pregnancy.** (A)

891 Human equivalent of murine CD122+Macs in first-trimester decidual tissue from 6-week elective

892 termination of pregnancy, stained with isotype control (left panel) or anti-CD122 (right panel).

893 Data are representative of 3 independent experiments. (B) Human CD122+Macs in first-trimester

894 decidual tissue, but not first-trimester chorionic villi, from 8-week elective termination of

895 pregnancy. Phenotypically, human CD122+Macs express many markers of the macrophage

896 lineage. Human CD122+Macs diverge from human cMacs by expressing high levels of CD122,

897 CD56, Perforin, and Granzyme B. Additional examples are shown in Supplemental Figure 2. (C)

898 Human CD122+Macs in secretory phase endometrium during the implantation window but not in

899 blood from the same subject. Additional examples are shown in Supplemental Figure 3.

900

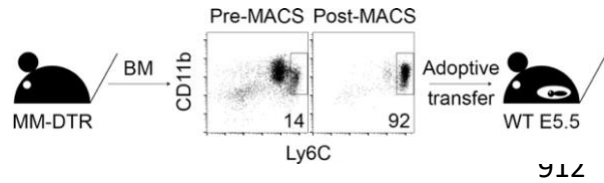
901

902

903
904
905
906
907

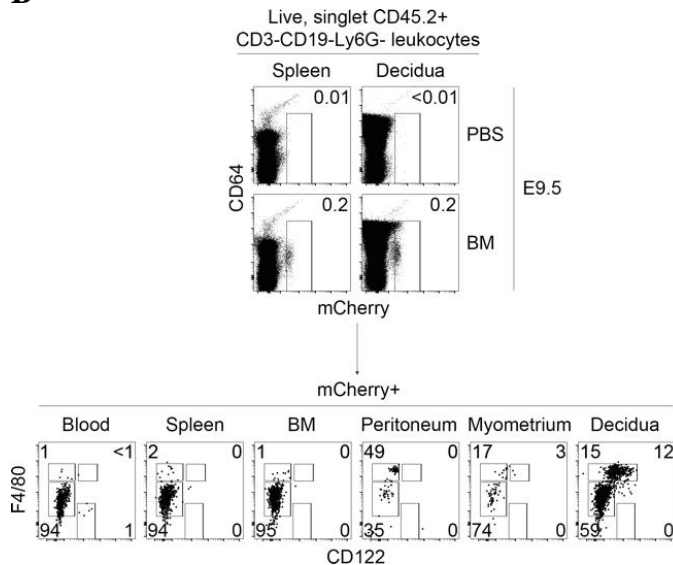
FIGURE 3

A



913
914

B



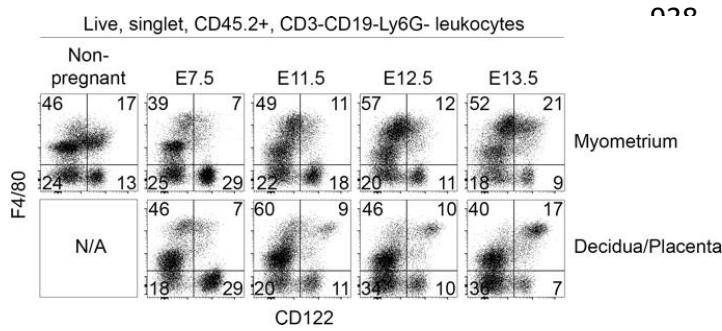
915
916
917
918
919
920
921
922
923
924
925
926
927
928
929
930
931
932
933
934

Figure 3. Bone marrow monocytes can give rise to CD122+Macs at the maternal-fetal interface during pregnancy. (A) Bone marrow monocytes from MM-DTR mice were enriched by magnetic-activated cell sorting (MACS) from non-pregnant mice prior to adoptive transfer into post-implantation pregnant mice. (B) Uterine CD122+Macs can derive from bone marrow (BM) monocytes. (Top panels) Four days after i.v. adoptive transfer of MM-DTR BM monocytes, mCherry+ (donor-derived) cells were recovered from recipients. Control mice received i.v. saline (PBS). Data are representative of at least 3 independent experiments with 2-3 recipients per experiment.

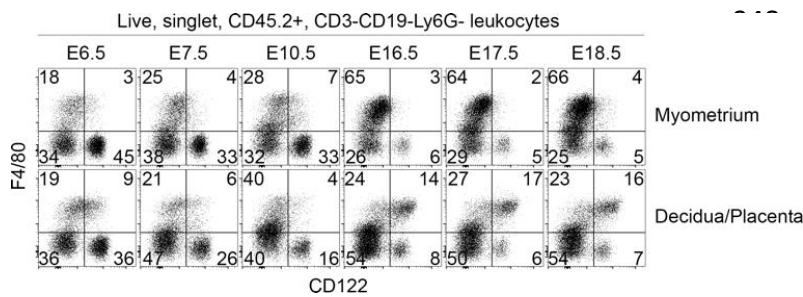
935 **FIGURE 4**

936

937 **A**

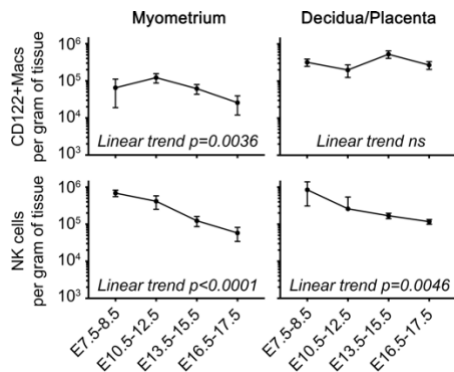


947 **B**



956

957 **C**



968

969 **Figure 4. Population dynamics of CD122+Macs differ between myometrium and deciduo-**

970 **placental unit.** (A, B) The myometrium is progressively enriched in CD122+Macs over the

971 course of gestation, until the sudden decline of CD122+Macs at E16.5 and beyond. The decidua

972 or combined deciduo-placental unit is progressively enriched in CD122+Macs as gestation

973 progresses toward term. “N/A”, not applicable. Data are representative of at least 3 independent

974 experiments with at least 3 total mice per timepoint. (C) Quantification of numbers of

975 CD122+Macs and NK cells per gram of indicated tissue shows that CD122+Macs decline over

976 gestation in the myometrium but remain constant in the decidua/placenta. NK cells decline over

977 time in both the myometrium and decidua/placenta. P values were generated by one-way ANOVA

978 with a test for linear trend and refers to whether the slope of each line (showing changes in cell

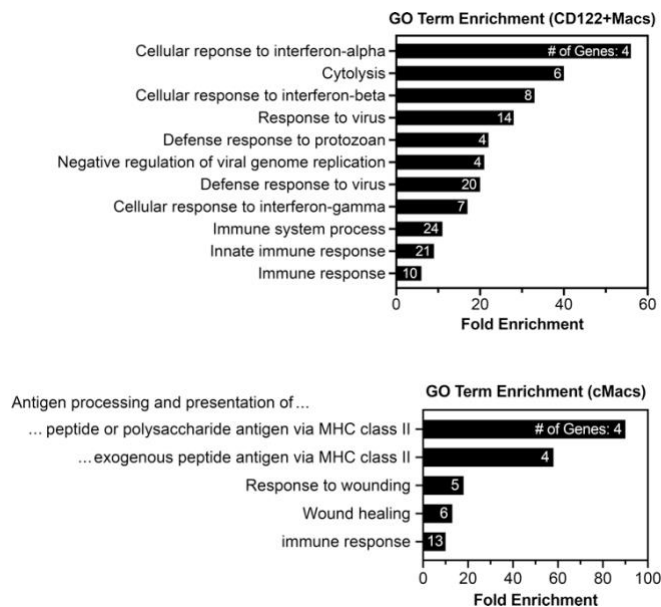
979 number per gram of tissue over time) was likely to have occurred by chance alone. “ns”, not

980 significant, p=0.38.

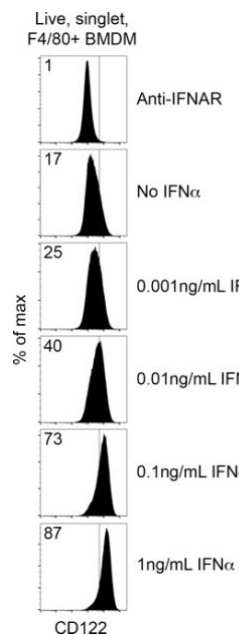
981
982
983
984
985

FIGURE 5

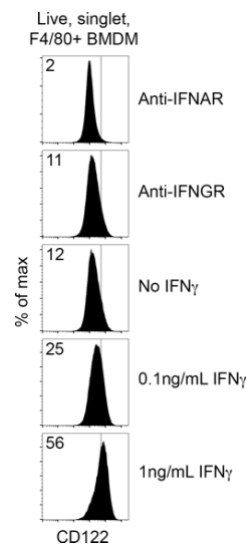
A



D

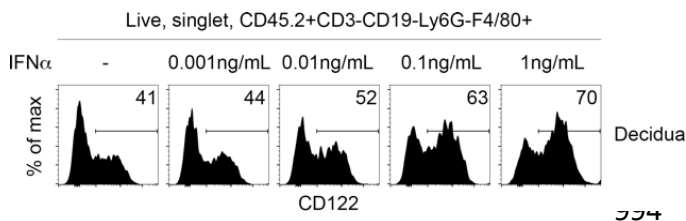


E



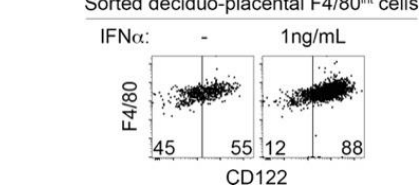
988

B



995

C



996

997

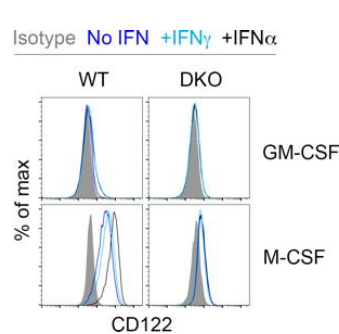
998

999

1000

1001

F

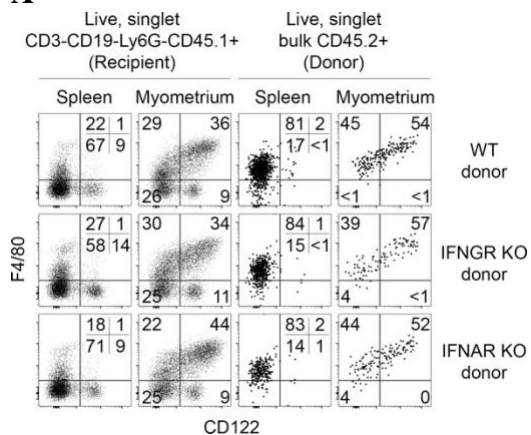


1002 **Figure 5. M-CSF and interferons drive expression of CD122 on uterine and bone marrow-**
1003 **derived macrophages.** (A) Interferon-responsive genes (ISGs) are overrepresented among genes
1004 significantly enriched in E7.5 decidual CD122+Macs relative to cMacs by microarray. Gene
1005 ontology (GO) analysis by DAVID of all genes significantly enriched in CD122+Macs relative to
1006 cMacs. Bars show fold enrichment for indicated GO Biological Process (GO BP) terms
1007 significantly enriched with FDR-adjusted $p < 0.05$. GO terms are represented by the number of
1008 genes shown in each bar. (B) Decidual F4/80+ cells upregulate CD122 in a dose-dependent
1009 fashion after 18hrs in culture with M-CSF and IFN α . Bulk E6.5 decidual cell suspensions were
1010 cultured in indicated concentrations of IFN α . Data are representative of 2 independent
1011 experiments. (C) Monocytes (CD122-F4/80_{int}) sort-purified from E15.5 decidua/placenta
1012 upregulate CD122 after 24 hours in culture with M-CSF and IFN α . Data are representative of 2
1013 independent experiments with 2-5 mice per experiment. (D, E) Dose-dependent upregulation of
1014 CD122 on bone marrow-derived macrophages (BMDMs) cultured with M-CSF and (D) Type-I
1015 IFN α or (E) Type-II IFN γ . Data are representative of at least 5 independent experiments. (F)
1016 Culture of bone marrow in M-CSF, not granulocyte/macrophage colony-stimulating factor (GM-
1017 CSF), permits induction of CD122 in response to IFN. M-CSF also drives modest expression of
1018 CD122 independent of IFN. “DKO” denotes IFNAR/IFNGR double KO mice. Data are
1019 representative of 3 independent experiments with 2-3 mice per group.
1020
1021
1022
1023

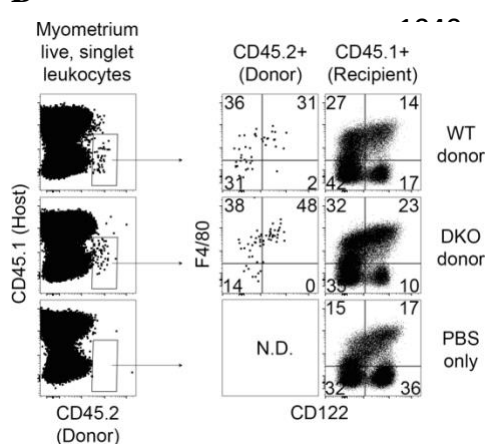
1024 **FIGURE 6**

1025

1026 **A**



1039 **B**



1052

1053

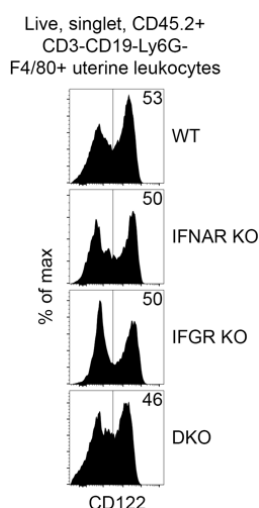
1054 **Figure 6. Neither Type I nor Type II IFN, alone or in combination, is required to generate**
 1055 **uterine CD122+Macs *in vivo*.** (A) MACS-enriched BM monocytes singly-deficient in either
 1056 Type-I IFN (IFNAR KO) or Type-II IFN receptor (IFNGR KO) are capable of giving rise to uterine
 1057 CD122+Macs. (B) MACS-enriched BM monocytes doubly-deficient in both IFNAR and IFNGR
 1058 KO (double KO, DKO) are capable of giving rise to uterine CD122+Macs. BM monocytes from
 1059 indicated non-pregnant donor mice (CD45.2+) were adoptively transferred into congenic
 1060 (CD45.1+) peri-implantation pregnant recipient mice. Indicated organs were analyzed at E15.5.
 1061 Late in gestation, transferred cells were recovered predominantly from myometrium and not from
 1062 decidua/placenta. Data are representative of 2-3 recipients from at least 2 independent
 1063 experiments. (C) Development of uterine CD122+Macs *in vivo* in non-pregnant wild-type, IFNAR
 1064 KO, IFNGR KO, and DKO mice. Data are representative of 4-6 total mice over 2 independent
 1065 experiments.

1066

1067

1068

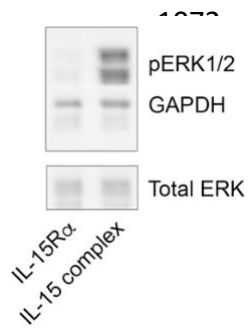
C



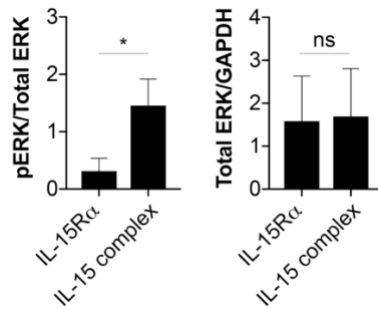
1069 **FIGURE 7**

1070

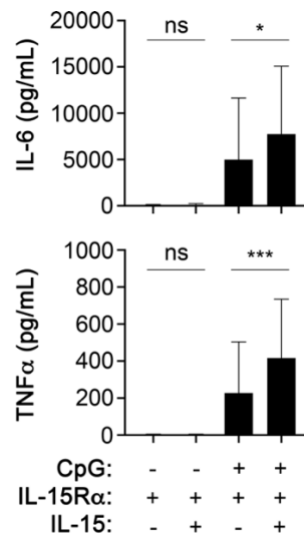
1071 **A**



B



C



1081

1082

1083

1084

1085

1086

1087

1088

1089 **Figure 7. CD122+Macs signal and exhibit enhanced function in response to IL-15.** (A)

1090 Phosphorylation of ERK1/2 (pERK1/2) by Western blot of CD122+BMDMs after 30 minutes of

1091 stimulation with IL-15 complex (recombinant murine IL-15 pre-complexed to recombinant murine

1092 IL-15Rα). “IL-15Rα” denotes addition of only recombinant IL-15Rα. (B) Increased pERK by

1093 Western is not due to increased total ERK. *, p=0.016 by the Wilcoxon matched-pairs signed rank

1094 test, includes 7 individual mice over 2 independent experiments. “ns”, not significant. (C)

1095 CD122+BMDMs co-stimulated with IL-15 complex and CpG produce more TNFα and IL-6 by

1096 ELISA than CD122+BMDMs stimulated with CpG alone. Here, presence of both IL-15Rα and

1097 IL-15 denotes use of IL-15 complex. BMDMs were stimulated for 16-24 hours, after which

1098 supernatants were collected for ELISA. *p=0.015 (top panel), ***p=0.0003 (bottom panel) by

1099 mixed-effects analysis (one-way ANOVA with paired observations) with Holm-Sidak’s multiple

1100 comparisons test. Bar graphs are compiled data from 11 biological replicates from 5 independent

1101 experiments, with BMDMs in triplicate generated from 1-3 individual mice per experiment. All

1102 individual data points, showing consistent response of BMDMs to IL-15 but variable response to

1103 CpG, are plotted in Supplemental Fig. 5.

1104

1105

1106

1107

1108